Available online at www.sciencedirect.com
SCIENCE DIRECT
Polymer 46 (2005) 10221–10225
polymer
www.elsevier.com/locate/polymer

All-cellulose nanocomposite

W. Gindl[a,*], J. Keckes[b]

[a]BOKU-Vienna, Department of Material Science and Process Engineering, A-1190 Vienna, Austria
[b]Erich Schmid Institute for Materials Science, Austrian Academy of Sciences, A-8700 Leoben, Austria

Received 8 August 2005; received in revised form 11 August 2005; accepted 13 August 2005
Available online 26 August 2005

Abstract

Cellulose-based nanocomposite films with different ratio of cellulose I and II were produced by means of partial dissolution of microcrystalline cellulose powder in lithium chloride/*N*,*N*-dimethylacetamide and subsequent film casting. The mechanical and structural properties of the films were characterised using tensile tests and X-ray diffraction. The films are isotropic, transparent to visible light, highly crystalline, and contain different amounts of undissolved cellulose I crystallites in a matrix of regenerated cellulose. The results show that, by varying the cellulose I and II ratio, the mechanical performance of the nanocomposites can be tuned. Depending on the composition, a tensile strength up to 240 MPa, an elastic modulus of 13.1 GPa, and a failure strain of 8.6% were observed. Moreover, the nanocomposites clearly surpass the mechanical properties of most comparable cellulosic materials, their greatest advantage being the fact that they are fully biobased and biodegradable, but also of relatively high strength.

Keywords: Cellulose; Nanocomposite; Self-reinforcement

1. Introduction

The importance of 'green' properties such as biodegradability and favourable CO_2 balance grows with the awareness of consumers and engineers for sustainability in the use of materials [1]. Reinforcement of polymer composites with plant fibre instead of glass fibre is a way of improving these properties, yet such composites are often of modest strength when both fibre and matrix are biobased and biodegradable [2–4].

Cellulosic fibre from wood, annual plants, and agricultural by-products is an abundant renewable resource [5,6]. Cellulose is a straight carbohydrate polymer chain consisting of several 1000 β 1–4 glucopyranose units. In cellulosic plant fibres, cellulose is present in amorphous state, but also associates to crystalline domains through intramolecular hydrogen bonding [7]. The elastic modulus of the cellulose I crystallite, which is the crystalline cellulose form typical for plant fibres, has been measured to 128 GPa [8], and estimates for the strength of the cellulose I crystallite lie in the order of 10 GPa [9]. In spite of the good mechanical properties of cellulose, the strength of cellulosic fibre-reinforced composites remains far below the potential provided by cellulose. Due to the heterogeneous structure and composition of plant fibres [10], and insufficient fibre-matrix compatibility [11–14], typical random-oriented plant fibre-reinforced composites show a tensile strength of 15–140 MPa and an elastic modulus of 1–13 GPa [15–20].

Recently, cellulose fibre-reinforced phenol–formaldehyde composites with high bending strength of up to 400 MPa were produced using cellulose nanofibrils obtained by microfibrillation of wood pulp [21] or from bacterial cellulose [22]. High-strength cellulosic composites were also obtained by self-reinforcement, embedding unidirectionally aligned ramie fibres in a matrix of regenerated cellulose [23]. Being chemically homogeneous, self-reinforced composites are easy to recycle.

In this study, we aim to combine advantages of nanofibre reinforcement and self-reinforcement in order to obtain high-strength random-oriented biobased, easily recyclable and biodegradable composites. For this purpose, microcrystalline cellulose will be partly dissolved in lithium chloride/*N*,*N*-dimethylacetamide solvent and films will be

* Corresponding author. Tel.: +43 1 47654 4255; fax: +43 1 47654 4295.
E-mail address: wolfgang.gindl@boku.ac.at (W. Gindl).

0032-3861/$ - see front matter © 2005 Elsevier Ltd. All rights reserved.
doi:10.1016/j.polymer.2005.08.040

cast from the solution. Tensile tests and X-ray diffraction will be used to characterise the films and evaluate the reinforcing effect of microcrystalline cellulose.

2. Materials and methods

2.1. Production of all-cellulose composite films

Aldrich microcrystalline cellulose (31,069-7, MCC) was chosen as raw material for the production of all-cellulose films. This microcrystalline powder (Fig. 1) is produced by acid hydrolysis of amorphous domains in cotton linters, which results in high crystallinity (~65%). MCC (2 g for composite A, 3 g for composite B, and 4 g for composite C) was activated for 6 h in distilled H_2O at room temperature. Subsequently, the cellulose was dehydrated in ethanol, acetone, and *N*,*N*-dimethylacetamide (DMAc) for 4 h each. In parallel, a solution of 8 g LiCl in 100 ml DMAc was prepared. After decanting DMAc from the dehydrated cellulose, 100 ml LiCl/DMAc solution was poured onto each of the three cellulose samples A (2 g MCC), B (3 g MCC), and C (4 g MCC) and stirred for 5 min. The solutions were then poured into Petri disks (diameter = 20 cm), and left at ambient atmosphere for 12 h. After this time a 5–8 mm thick transparent gel had formed which was washed in distilled water and dehydrated between gently compressed sheets of paper. The final films were optically transparent and had a thickness between 0.2 and 0.5 mm.

In order to evaluate the reinforcing effect of microcrystalline cellulose, pure isotropic regenerated cellulose was chosen as a reference material. Regenerated cellulose films were produced by dissolving 1 g lyocell fibres for 24 h in 100 ml LiCl/DMAc under constant stirring at room temperature. The solution was poured into a Petri disk and left in ambient atmosphere as described above. Thereafter, the regenerated cellulose film was dehydrated between sheets of paper, resulting in a final film thickness of 0.2 mm.

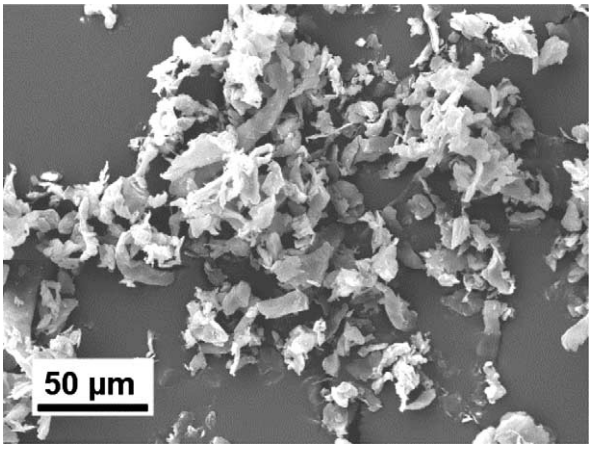

Fig. 1. SEM image of microcrystalline cellulose powder (cotton linters).

2.2. Structural characterisation

Tensile tests were performed using strips of cellulose film with a length of 100 mm and a width of 7 mm. Before testing, all specimens were equilibrated in a chamber kept at 20 °C and 65% relative humidity. Samples were strained at a cross-head displacement rate of 1 mm min^{-1} on a Zwick 20 kN universal testing machine equipped with a Zwick-macrosense clip-on strain measuring device.

The structural properties of the films were characterised using X-ray diffraction. At first, $\theta/2\theta$ measurements were performed using a powder diffractometer D8Advance working with Cu Kα radiation, energy dispersive detector and Göbel mirrors. Crystallinity was determined from the ratio of crystalline scattering versus total scattering, whereby the amorphous contribution was estimated by polynomial approximation [24]. The preferred orientation in the films was characterised using a system Nanostar (Bruker AXS) connected to a rotating anode generator with Cu target. The system is equipped with crossed Göbel mirrors, a pinhole system for a primary collimation with a beam diameter of 100 µm and a two-dimensional (2D) wire detector (Hi-Star).

Finally, transmittance to visible light was measured by placing the films in a Zeiss MPM800 spectrophotometer microscope. Using a circular measuring spot of 3 mm in diameter, spectra were in steps of 5 nm between 400 and 700 nm. The transmittance of a commercial microscope glass slide with 0.5 mm thickness was taken as a reference.

3. Results and discussion

3.1. Structural characterisation

The term all-cellulose composite was first introduced by Nishino et al. [23] for a material consisting of ramie fibres embedded in a matrix of regenerated cellulose. The films obtained in the present study by partly dissolving MCC in LiCl/DMAc are referred to as composites because regenerated cellulose is supposed to serve as matrix, which is reinforced by cellulose I crystallites originating from undissolved MCC. Although regenerated cellulose and reinforcing crystallites are chemically identical, the term 'composite' is considered appropriate since the two components exhibit different structure and different mechanical properties [8].

Wide angle X-ray scattering detector images of all-cellulose composite films are shown in Fig. 2. The constant equatorial distribution of scattering intensity in rings corresponding to different crystalline reflections indicates a perfectly random orientation of crystallites. $\theta/2\theta$ scans (Fig. 3) give an insight into the crystalline structure of the films. The intensity distribution of regenerated cellulose sheets formed from 1 g Lyocell fibres dissolved in LICl/DMAc indicates that the crystalline part of this film is cellulose II [25], which shows highest scattering intensity at

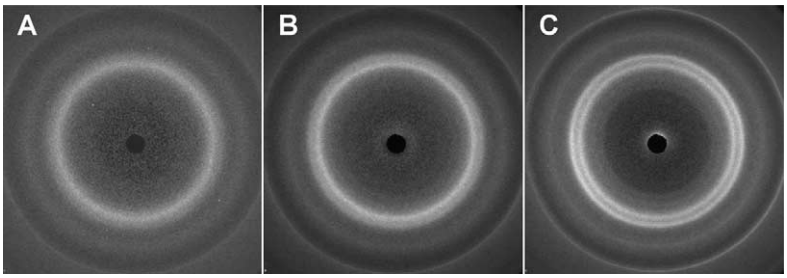

Fig. 2. WAXS of dried all-cellulose composite films type A, B, and C produced by partly dissolving different amounts of MCC in 100 ml LiCl/DMAc, indicating isotropic nature and a different composition.

an angle of 20.4° (Fig. 3). By contrast, the crystalline part of MCC powder corresponds to cellulose I [26] and shows highest scattering intensity at 22.7°. A comparison of $\theta/2\theta$ scans obtained from composites A, B, and C made by partly dissolving different amounts of MCC in LiCl/DMAc reveals differences in crystallinity and cellulose I/cellulose II content. Composite A is very similar to regenerated cellulose, apart from a slight shoulder at a scattering angle of 22.7° indicating the presence of cellulose I. This shoulder becomes more prominent in composite B and finally develops into a clear intensity peak in composite C. The ratio of scattering intensity at 22.7° vs. intensity at 20.4° ($I_{22.7°}/I_{20.4°}$) is indicative of cellulose I vs. cellulose II content. $I_{22.7°}/I_{20.4°}$ is 0.71 in regenerated cellulose and 1.22 in MCC. In composites A, B, and C, this ratio increases from 0.83 to 0.93, and to 1.01, respectively (Table 1). The progressive increase of the ratio $I_{22.7°}/I_{20.4°}$ may be interpreted as an increase in the proportion of cellulose I crystallites with respect to cellulose II crystallites.

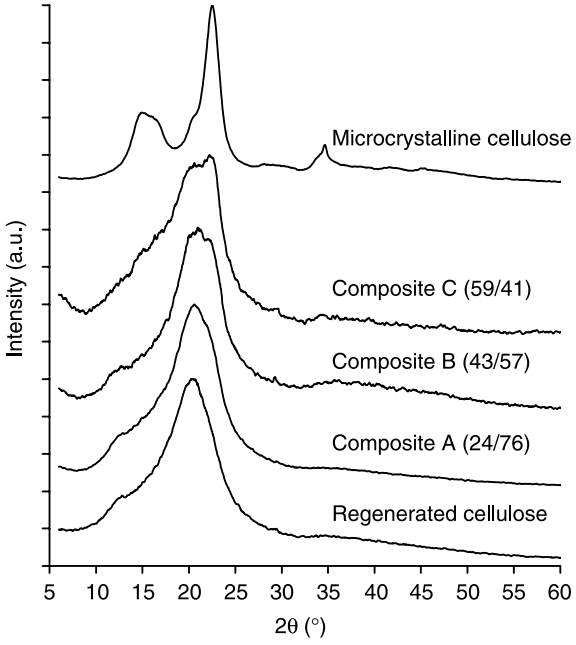

Fig. 3. XRD powder diffraction data from microcrystalline cellulose, regenerated cellulose, and all-cellulose composites with varying content of cellulose I and cellulose II. Numbers in brackets denote the estimated cellulose I/cellulose II ratio.

Assuming a linear relationship between the ratio $I_{22.7°}/I_{20.4°}$ and cellulose I/cellulose II content, a rough estimate of the latter was calculated (Table 1). Based on this estimate, which considers only the peak height of the respective most intense reflection, the cellulose I part of the crystalline cellulose in the composites increases from 24% in composite A to 59% in composite C. This signifies that with an increase in the amount of MCC powder added to a constant volume (100 ml) of LiCl/DMAc solution (Table 1), progressively less MCC was dissolved and transformed into regenerated cellulose. Increasing amounts of cellulose I remained undissolved in composites A, B, and C, serving as reinforcement of the regenerated cellulose matrix. In addition to the type of crystallite, overall crystallinity of the composite films was also different. Sheets of regenerated cellulose were 39% crystalline. In the composites A, B, and C, crystallinity was 46, 52, and 57%, respectively (Table 1). This corresponds well to the fact that increasing amounts of highly crystalline MCC remained undissolved in the production of composites A, B, and C, thus increasing overall crystallinity. Presumably the short stirring in LiCl/DMAc solution of only 5 min led to the preferred dissolution of non-crystalline domains in MCC, while crystalline domains remained largely unaffected. The lateral dimensions of cellulose crystallites in the composite films were evaluated by means of the Scherrer formula and typically are in the range of 1–3.5 nm. Thus we refer to the all-cellulose films produced here as nanocomposites of regenerated cellulose reinforced by cellulose I crystallites. This statement is supported by the fact that the all-cellulose composite films A, B, and C show excellent transparency to visible light (Fig. 4). Since only components less than 1/10 of a wavelength in size provide optical transparency [27], we presume that only nanoscale components are present in our all-cellulose composite films. Optical transparency also requires a perfect bonding between matrix and fibre, which goes in line with the fact that no signal could be detected in tentative small angle X-ray scattering experiments with our all-cellulose composite films.

3.2. Mechanical testing

Tensile tests of pure regenerated cellulose and all-cellulose nanocomposite films A, B, and C revealed an

Table 1
Results of tensile tests and X-ray diffraction with films of all-cellulose nanocomposite films produced using different amounts of MCC added to 100 ml LiCl/DMAc solvent compared to pure regenerated cellulose

Material	Amount of MCC (g)	Elastic modulus (GPa)	Tensile strength (MPa)	Failure strain (%)	Crystallinity (%)	$I_{22.7°}/I_{20.4°}$	Cellulose I/ Cellulose II
Regenerated cellulose	–	6.9	170.3	18.2	39	0.71	–
Composite A	2	12.6	218.6	10.7	46	0.83	24/76
Composite B	3	13.1	242.8	8.6	52	0.93	43/57
Composite C	4	14.9	215.1	3.6	57	1.01	59/41

increase in the elastic modulus and a decrease in failure strain concurrent with increasing crystallinity and cellulose I/cellulose II ratio (Fig. 5, Table 1). Tensile strength also increased considerably with respect to regenerated cellulose, and reached maximum values for composite B (243 MPa). In an extensive review, Fink et al. [28] compared properties of new high performance extrusion blown regenerated cellulose films with cellophane. While the tensile strength of cellophane was 125 MPa in longitudinal- and 75 MPa in transversal direction, extrusion blown films showed 100–300 MPa longitudinally and 50–200 MPa transversally, depending on the degree of anisotropy in cellulose chain orientation achieved by varying production parameters. In the case of balanced longitudinal and transversal drawing ratio, chain orientation was close to, but not fully isotropic, in which case tensile strength was 114 MPa longitudinally and 82 MPa transversally. This indicates that in the case of in-plane isotropic orientation, all-cellulosic nanocomposite films produced here surpass the tensile strength of extrusion blown films and cellophane by a factor 2. Also regarding their elastic modulus, composite B with 13.1 GPa is highly competitive with extrusion blown films (2–8 GPa depending on orientation anisotropy) and cellophane (3.7–5.4 GPa).

In addition to regenerated cellulose films, recently introduced all-cellulose composites [23] may also serve as reference for our all-cellulose nanocomposite films. Composites presented by Nishino et al. [23] consist of a high proportion of unidirectionally aligned ramie fibres embedded in a matrix of regenerated cellulose. The tensile strength of this composite was 480 MPa. Assuming that a change to in-plane random fibre orientation will reduce strength to roughly a third of the strength measured at unidirectional fibre alignment, a hypothetical strength of 160 MPa may be assumed for a random-oriented ramie fibre-reinforced all-cellulose composite. Considering this, our all-cellulose nanocomposite films with tensile strength up to 240 MPa compare very favourably with ramie fibre-reinforced all-cellulose composites.

The nanocomposite films presented here are a new class of composite materials within the variety of nanoscale reinforced materials based on cellulosic whiskers [3] and microfibrillated cellulose [2,4,21,29]. While based entirely on cellulose and therefore fully biodegradable [30], all-cellulose nanocomposite films surpass the mechanical properties of most comparable random-oriented composite materials published, with the notable exception of composites based on microfibrillated cellulose [21] and bacterial cellulose [22]. Future experiments will aim at a combination of the reinforcement efficiency of the latter fibres, which show superior aspect ratio compared to microcrystalline cellulose, with the superior matrix properties achievable by cellulose self-reinforcement.

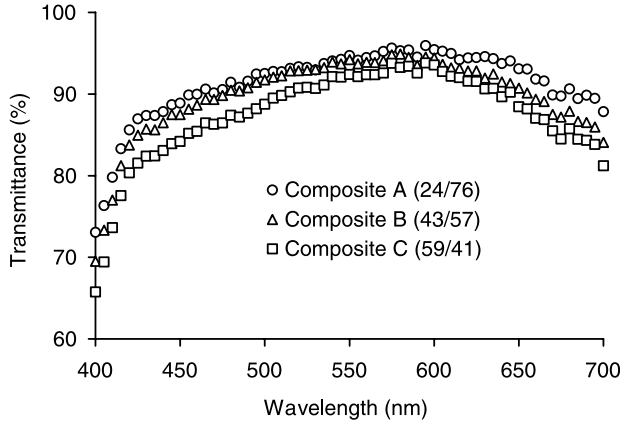

Fig. 4. Transmittance of all-cellulose films to visible light. Numbers in brackets denote the estimated cellulose I/cellulose II ratio.

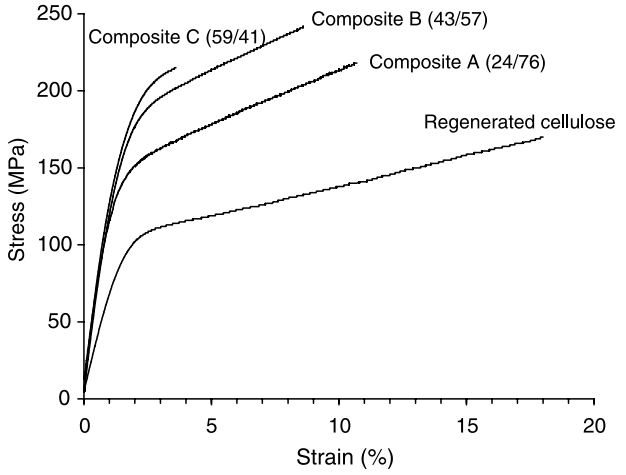

Fig. 5. Stress strain graphs from tensile tests of all-cellulose composites A, B, and C, and regenerated cellulose. Numbers in brackets denote the estimated cellulose I/cellulose II ratio.

4. Conclusion

It is shown that by means of partial dissolution of microcrystalline cellulose powder in LiCl/DMAc and subsequent film casting, all-cellulose nanocomposite films consisting of regenerated cellulose reinforced with undissolved cellulose I crystallites can be produced. Such random-oriented nanocrystallite reinforced films are transparent to visible light and of high strength and stiffness with regard to comparable cellulosic materials. However, the biggest advantage of the new nanocomposite films is the fact that they are at the same time fully biobased, easily recyclable and biodegradable, yet reasonably strong materials.

References

[1] Netravali AN, Chabba S. Mater Today 2003;6:22–9.
[2] Hepworth DG, Bruce DM. Composites Part A 2000;31:283–5.
[3] Azizi-Samir AS, Alloin F, Dufresne A. Biomacromolecules 2005;6:612–26.
[4] Zimmermann T, Pöhler E, Geiger T. Adv Eng Mater 2004;6:754–61.
[5] Eichhorn SJ, Baillie CA, Zafeiropoulos N, Mwaikambo LY, Ansell MP, Dufresne A, et al. J Mater Sci 2001;36:2107–31.
[6] Reddy N, Yang Y. Trends Biotechnol 2005;23:22–7.
[7] Klemm D, Heublein B, Fink H-P, Bohn A. Angew Chem Int Ed 2005;44:2–37.
[8] Nishino T, Takano K, Nakamae KJ. Polym Sci B 1995;33:1647–51.
[9] Azizi-Samir AS, Alloin F, Paillet M, Dufresne A. Macromolecules 2004;37:4313–6.
[10] Bledzki AK, Gassan J. Prog Polym Sci 1999;24:221–74.
[11] Felix JM, Gatenholm P. J Appl Polym Sci 1991;42:609–20.
[12] Wu J, Yu D, Chan C-M, Kim J, Mai Y-W. J Appl Polym Sci 2000;76:1000–10.
[13] Ichazo MN, Albano C, González J, Perera R, Candal MV. Compos Struct 2001;54:207–14.
[14] Colom X, Carrasco F, Pagès P, Canavete J. Compos Sci Technol 2003;63:161–9.
[15] Hua L, Zadorecki P, Flodin P. Polym Compos 1987;8:199–202.
[16] Caulfield DF, Feng D, Prabawa S, Young RA, Sanadi AR. Angew Makromol Chem 1999;272:57–64.
[17] Glasser WG, Taib R, Jain RK, Kander R. J Appl Polym Sci 1999;73:1329–40.
[18] Hughes M, Hill CAS, Hague JRB. J Mater Sci 2002;37:4669–76.
[19] Lundquist L, Marque B, Hagstrand PO, Leterrier Y, Manson JAE. Compos Sci Technol 2003;63:137–52.
[20] Gindl W, Jeronimidis G. J Mater Sci 2004;39:3245–7.
[21] Nakagaito AN, Yano H. Appl Phys A 2003;80:155–9.
[22] Nakagaito AN, Iwamoto S, Yano H. Appl Phys A 2005;80:93–7.
[23] Nishino T, Matsuda I, Hirao K. Macromolecules 2004;37:7683–7.
[24] Smole MS, Persin Z, Kreze T, Kleinschek KS, Ribitsch V, Neumayer S. Mater Res Innovations 2003;7:275–82.
[25] Fink HP, Fanter D, Philipp B. Acta Polym 1985;36(1):8.
[26] Wada M, Sugiyama J, Okano T. J Appl Polym Sci 1993;49:1491–6.
[27] Yano H, Sugiyama J, Nakagaito AN, Nogi M, Matsuura T, Hikita M, et al. Adv Mater 2005;17:153–5.
[28] Fink HP, Weigel P, Purz HJ, Ganster J. Prog Polym Sci 2001;26:1473–524.
[29] Berglund L. Cellulose-based nanocomposites. In: Mohanty AK, Misra M, Drzal LT, editors. Natural fibers, bioploymers, and biocomposites. Boca Raton: Taylor and Francis; 2005. p. 807–32.
[30] Mohanty AK, Misra M, Drzal LT, Selke SE, Harte BR, Hinrichsen G. Natural fibers, biopolymers, and biocomposites: An introduction. In: Mohanty AK, Misra M, Drzal LT, editors. Natural fibers, bioploymers, and biocomposites. Boca Raton: Taylor and Francis; 2005. p. 1–36.